



## ORIGINAL ARTICLE

# Investigation into the adsorption of CO<sub>2</sub>, N<sub>2</sub> and CH<sub>4</sub> on kaolinite clay



Xidong Du <sup>a</sup>, Dongdong Pang <sup>b,\*</sup>, Yuan Zhao <sup>c,d</sup>, Zhenkun Hou <sup>e</sup>, Hanglong Wang <sup>a</sup>, Yugang Cheng <sup>f</sup>

<sup>a</sup> Yunnan Key Laboratory of Sino-German Blue Mining and Utilization of Special Underground Space, Faculty of Land Resources Engineering, Kunming University of Science and Technology, Kunming, Yunnan 650093, China

<sup>b</sup> Key Laboratory of Safety and High-efficiency Coal Mining, Ministry of Education (Anhui University of Science and Technology), Huainan 232001, China

<sup>c</sup> Sinohydro Engineering Bureau 8 Co. LTD., POWERCHINA, Changsha 410004, China

<sup>d</sup> Department of Hydraulic Engineering, Tsinghua University, Beijing 100084, China

<sup>e</sup> School of Civil and Transportation Engineering, Guangdong University of Technology, Guangzhou, Guangdong 510006, China

<sup>f</sup> State Key Laboratory of Mountain Bridge and Tunnel Engineering, Chongqing Jiaotong University, Chongqing 400074, China

Received 10 September 2021; accepted 20 December 2021

Available online 30 December 2021

## KEYWORDS

Adsorption;  
Shale gas;  
Kaolinite;  
Thermodynamics;  
CO<sub>2</sub> sequestration

**Abstract** Investigating the adsorption characteristics of CO<sub>2</sub>, N<sub>2</sub> and CH<sub>4</sub> on kaolinite clay is beneficial for enhanced shale gas recovery by gas injection. In this paper, the experiments of CO<sub>2</sub>, N<sub>2</sub> and CH<sub>4</sub> adsorption at 288 K, 308 K and 328 K on kaolinite clay were conducted, and the thermodynamics analysis of adsorption of three gases was performed. The findings reveal that the order of the uptakes of three gases on kaolinite clay is as follows: N<sub>2</sub> < CH<sub>4</sub> < CO<sub>2</sub>. Reducing temperature enlarges the separation coefficients of CO<sub>2</sub> over CH<sub>4</sub> ( $\alpha_{\text{CO}_2/\text{CH}_4}$ ), CO<sub>2</sub> over N<sub>2</sub> ( $\alpha_{\text{CO}_2/\text{N}_2}$ ), and CH<sub>4</sub> over N<sub>2</sub> ( $\alpha_{\text{CH}_4/\text{N}_2}$ ). The value of  $\alpha_{\text{CO}_2/\text{CH}_4}$  greater than one validates that CO<sub>2</sub> is capable to directly replace the pre-adsorbed CH<sub>4</sub>. The spontaneity of CO<sub>2</sub> adsorption is the highest, while N<sub>2</sub> has the lowest adsorption spontaneity. Injecting N<sub>2</sub> into gas-bearing reservoir can cause CH<sub>4</sub> desorption by lowering the spontaneity of CH<sub>4</sub> adsorption. Adsorbed CO<sub>2</sub> molecules form a most ordered rearrangement on kaolinite surface. The decrease rate of entropy loss for N<sub>2</sub> adsorption is higher than those for CO<sub>2</sub> and CH<sub>4</sub> adsorption.

© 2021 The Author(s). Published by Elsevier B.V. on behalf of King Saud University. This is an open access article under the CC BY-NC-ND license (<http://creativecommons.org/licenses/by-nc-nd/4.0/>).

\* Corresponding author.

E-mail address: [PangDD1989@126.com](mailto:PangDD1989@126.com) (D. Pang).

Peer review under responsibility of King Saud University.



Production and hosting by Elsevier

## 1. Introduction

Urgent demand for natural gas resources has stimulated the exploitation of unconventional gas, such as shale gas, coalbed gas and tight gas (Du et al., 2018, 2021a; Huang et al., 2018). Shale gas, occurring as free gas in pore fracture network or adsorbed gas on the matrix surface, has increasingly considered as the significant alternative for conventional gas (Du et al., 2017, 2019a, Qin et al., 2021a,b). At present, CO<sub>2</sub>

geological sequestration is one of the most prospective techniques for the reduction of CO<sub>2</sub> emissions. Given that the higher adsorption capacity of CO<sub>2</sub> over CH<sub>4</sub> on shale reservoir, utilization of CO<sub>2</sub> can promote the recovery of additional CH<sub>4</sub> from gas shale formations with an added benefit of the creation of valuable sequestration option for greenhouse gas. Meanwhile, the injection of N<sub>2</sub> into gas-bearing sediments also has the ability to trigger the desorption of substantial amounts of adsorbed CH<sub>4</sub> by reducing CH<sub>4</sub> partial pressure and breaking the equilibrium condition, and taking N<sub>2</sub> as injection agent is also effective to improve gas production (Jessen et al., 2008). Therefore, owing to the feasibility, recovery cost and environment remediation, the technologies of enhanced shale gas recovery using CO<sub>2</sub> (CO<sub>2</sub>-ESGR) and N<sub>2</sub> (N<sub>2</sub>-ESGR) have gained lots of attentions (Du et al., 2019b; Huo et al., 2017; Liu et al., 2019; Zhao et al., 2020).

For shale reservoir, inorganic minerals and organic matter are the two main distinct media. As the important component of inorganic minerals, clay minerals have a remarkable effect on the adsorption and migration properties of fluids due to the larger surface area and complex pore structure (Jin and Firoozabadi, 2014). To optimize the implementation strategy of enhanced hydrocarbon recovery by gas injection, the reliable and accurate adsorption equilibrium data of CO<sub>2</sub>, N<sub>2</sub> and CH<sub>4</sub> on clay minerals (kaolinite, montmorillonite and illite) over a broad range of pressures and temperatures are necessary. Among the clay minerals, kaolinite clay is very common within shale formation (Zhang et al., 2018). Especially for some kaolinite-rich shale reservoir, the influence of kaolinite clay on fluid adsorption is significant. Therefore, comprehending the adsorption behaviors of fluids on kaolinite clay is meaningful for shale gas development and CO<sub>2</sub> sequestration.

Recently, many contributions have been conducted to study the fluid adsorption on kaolinite clay by laboratory experiment and molecular simulation. For example, Heller and Zoback (2014) measured the isothermal sorption curves of CH<sub>4</sub> and CO<sub>2</sub> on kaolinite clay and discovered that the adsorption capacity of CO<sub>2</sub> is obviously higher than that of CH<sub>4</sub>. Song et al. (2018) used molecular simulation method to investigate the effect of pore size on the adsorption of CH<sub>4</sub> and CO<sub>2</sub>. They found that the uptakes of CH<sub>4</sub> and CO<sub>2</sub> on kaolinite clay both decrease with increasing pore size. Zhou et al. (2019) researched the competitive sorption behaviors of injected CO<sub>2</sub> and pre-adsorbed CH<sub>4</sub> through molecular simulation. Their results showed that CH<sub>4</sub> adsorption on kaolinite clay can be obviously suppressed by injected CO<sub>2</sub>. Kang et al. (2020) analyzed the influences of temperature and pressure on CH<sub>4</sub>/CO<sub>2</sub> adsorption on kaolinite clay and indicated that the interaction of CH<sub>4</sub> with kaolinite is much lower than that of CO<sub>2</sub> with kaolinite. Evidently, the relevant researches about fluid adsorption on kaolinite clay mainly report CH<sub>4</sub> and CO<sub>2</sub> equilibrium adsorption data. The physical interaction of N<sub>2</sub> with kaolinite clay receives less attention, and the available equilibrium data for N<sub>2</sub> adsorption on kaolinite clay remains quite scattered. Therefore, it is needed to thoroughly study the interaction of N<sub>2</sub> and kaolinite clay and systematically compare the sorption characteristics of CO<sub>2</sub>, N<sub>2</sub> and CH<sub>4</sub> on kaolinite clay.

The better understanding of fluid adsorption on clay minerals must be relied on thermodynamics. Many thermodynamics variables can provide valuable physical sense to explain the interaction of adsorbent-adsorbate systems (Du et al., 2020b). The investigation about the sorption characteristics of CO<sub>2</sub>, N<sub>2</sub> and CH<sub>4</sub> on kaolinite clay also needs to take entropy loss ( $\Delta S$ ), surface potential ( $\Delta\Omega$ ), enthalpy change ( $\Delta H$ ), change of Gibbs free energy ( $\Delta G$ ) and isosteric heat of adsorption ( $Q_{st}$ ) into consideration. Hitherto, the published literatures are concentrated on  $Q_{st}$  of CH<sub>4</sub> on kaolinite clay, neglecting the equally important parameters of  $\Delta S$ ,  $\Delta\Omega$  and  $\Delta G$  (Xiong et al., 2017; Zhang et al., 2018). Meanwhile, the studies about CO<sub>2</sub> and N<sub>2</sub> adsorption on kaolinite clay from the point of view of thermodynamics are very lacking. Therefore, to better understand the adsorption mechanism of three gases on kaolinite clay, it is necessary to perform the thermodynamics analysis of CO<sub>2</sub>, N<sub>2</sub> and CH<sub>4</sub> adsorption.

The purpose of the current work is to compare the adsorption behaviors and investigate the competitive adsorption mechanism of CO<sub>2</sub>, N<sub>2</sub> and CH<sub>4</sub> on kaolinite clay. To address this issue, we report the adsorption measurements conducted on kaolinite clay with CO<sub>2</sub>, N<sub>2</sub> and CH<sub>4</sub> at 288–328 K. The thermodynamics variables of  $Q_{st}$ ,  $\Delta\Omega$ ,  $\Delta G$  and  $\Delta S$  of three gases were discussed. We hope that the findings can serve as a foundation for the research of shale gas exploration and CO<sub>2</sub> geological storage in kaolinite-rich shale formations.

## 2. Materials

The kaolinite clay was sourced from Shanghai Macklin Biochemical Technology Co., Ltd (Shanghai, China). The three gases adopted in this research were acquired from Tiange Gas Co., Ltd (Chongqing, China) at the purities of 99.999% for CH<sub>4</sub>, 99.999% for CO<sub>2</sub> and 99.99% for N<sub>2</sub>.

## 3. Experiments

### 3.1. Microscopic structural characterization

The pysisorption of low-pressure CO<sub>2</sub> and N<sub>2</sub> using an ASAP 2460 analyzer (Micromeritics, Georgia, USA) was performed to obtain the microscopic structure of kaolinite clay. Due to the pore shrinkage effect at ultra-low temperature of 77 K, N<sub>2</sub> molecule cannot enter into the ultrafine pore space (Wang et al., 2015). On the contrary, CO<sub>2</sub> molecule has the ability to diffuse into smaller micropore. Thereby, CO<sub>2</sub> molecule can more accurately probe the micropore information, and the micropore morphology of kaolinite clay was determined by low-pressure CO<sub>2</sub> adsorption. The low-pressure N<sub>2</sub> adsorption was adopted to provide the mesopore and macropore properties of kaolinite clay. According to the obtained adsorption data, the pore size distribution, pore volume and specific surface area can be determined.

### 3.2. Adsorption isotherm measurement

The adsorption isotherm measurements for CO<sub>2</sub>, N<sub>2</sub> and CH<sub>4</sub> were conducted using a high-resolution gravimetric analyzer (IGA-100B, U.K.). Unlike the traditional volumetric method, gravimetric method is a direct experiment method to measure the adsorption quantity. As demonstrated by Liu et al. (2019), for the isothermal adsorption measurement conducted on shale, gravimetric system has a higher accuracy than volumetric system. Hence, gravimetric method was chosen to conduct the adsorption experiments of CO<sub>2</sub>, N<sub>2</sub> and CH<sub>4</sub> on kaolinite clay.

In addition, due to the cation-exchange property of clay sheets and the full/partial changes of clay atoms, clay minerals always have the strong hydrophilicity (Wang and Huang, 2019). Accordingly, in order to remove the effect of moisture on the sorption performances of CO<sub>2</sub>, N<sub>2</sub> and CH<sub>4</sub> on kaolinite clay, the experiment system was degassed at 378 K for 10 h before the sorption measurement. Then, the experiment pressure was enhanced to the set value and the adsorption quantity versus time was automatically recorded. This experiment process was repeated until the maximum experiment pressure was reached.

## 4. Modeling

### 4.1. Adsorption model

The isothermal sorption curve can not only give insight into the adsorptive potential for an adsorbent but also provide the information about the surface properties of adsorbent and the interaction between adsorbate-adsorbent systems (Du et al., 2021b; Hameed et al., 2017; Kamboh et al., 2014; Song et al., 2017). At present, many adsorption models, such as Langmuir model, Brunauer-Emmett-Teller model and pore-filling model, have been proposed to model the adsorption isotherms (Tang et al., 2017). Among these models, Langmuir model is the most commonly used model based on the simplicity and the reasonable explanation to the model variables. Langmuir model assumes that the adsorption is occurring on the chemically, energetically and structurally homogeneous surface by monolayer sorption (Zhou et al., 2012). The isothermal sorption curves of CO<sub>2</sub>, N<sub>2</sub> and CH<sub>4</sub> were matched by Langmuir model. Eq. (1) gives the form of Langmuir model.

$$n = \frac{n_m b P}{1 + b P} \quad (1)$$

where  $n_m$  is the maximum monolayer adsorption amount;  $b$  is the Langmuir constant;  $n$  is the uptake; and  $P$  is pressure.

The fitness of Langmuir equation to experiment results can be analyzed by correlation coefficient ( $R^2$ ) and average relative error (ARE) (Song et al., 2017). The average relative error was calculated by Eq. (2).

$$ARE(\%) = \frac{100}{m} \sum_{i=1}^m \left| \frac{n_{\text{exp}} - n_{\text{mol}}}{n_{\text{exp}}} \right|_i \quad (2)$$

where  $n_{\text{mol}}$  is the simulated data; and  $n_{\text{exp}}$  is the testing data.

### 4.2. Separation coefficient

The separation coefficient can be used as an indicator to estimate the competitive adsorption of fluids on adsorbent (Merkel et al., 2015). A greater separation coefficient reveals that the difference in interaction strengths of fluids is more remarkable and the pre-adsorbed component with weaker adsorption can be easily and effectively replaced by the component with stronger adsorption. The separation coefficient is expressed by Eq. (3) (Song et al., 2017).

$$\alpha_{i/j} = \frac{n_{m,i} b_i}{n_{m,j} b_j} \quad (3)$$

where  $b_i$  and  $b_j$  are the Langmuir constants of component  $i$  and component  $j$ , respectively; and  $n_{m,i}$  and  $n_{m,j}$  are the maximum sorption capacities of component  $i$  and component  $j$ , respectively.

### 4.3. Henry's coefficient

When the experiment pressure is small, the adsorption quantity increases linearly with pressure, which is known as Henry's law (Tang et al., 2015). Over the Henry's region, each adsorbate molecule can be independently in contact with the whole material surface. The interaction force between adsorbate and

material surface is dominated at the low pressure condition (Du and Wang, 2021). Consequently, Henry's coefficient ( $K_H$ ) can be identified as a useful index to estimate the adsorption affinity. The larger  $K_H$  corresponds to the stronger adsorption affinity.

At the low-pressure region, the relation of uptake and pressure can be described by virial equation, as shown in Eq. (4) (Du et al., 2020a; Ning et al., 2012).

$$\ln((P/\text{MPa})/(q/\text{mmol/g})) = K_0 + K_1 n + K_2 n^2 + K_3 n^3 + \dots \quad (4)$$

where  $K_0$ ,  $K_1$ ,  $K_2$  and  $K_3$  are the first, second, third and fourth virial coefficients, respectively;  $K_0$  is related to Henry's coefficient, and  $K_H = \exp(-K_0)$ .

Considering the smaller adsorption amount, the higher-order term in Eq. (4) can be removed, and Eq. (5) can be gained.

$$\ln((P/\text{MPa})/(q/\text{mmol/g})) = K_0 + K_1 n \quad (5)$$

Through matching the linear part of  $\ln(P/q)$  as a function of  $n$ ,  $K_0$  can be acquired, and then  $K_H$  can be calculated.

### 4.4. Adsorption thermodynamics

The main thermodynamics parameters discussed in this work are  $Q_{st}$ ,  $\Delta\Omega$ ,  $\Delta G$  and  $\Delta S$ .  $Q_{st}$  is important in assessing the heat evolved/consumed during the adsorption/desorption processes (Sircar, 1992).  $Q_{st}$  at a given uptake ( $q_i$ ) can be calculated using Clausius-Clapeyron equation, as expressed in Eq. (6) and Eq. (7) (Xue et al., 2018).

$$Q_{st} = RT^2 \left( \frac{\partial \ln(P/\text{MPa})}{\partial T} \right)_{n_i} \quad (6)$$

$$\ln(P/\text{MPa}) = -\frac{Q_{st}}{RT} + C \quad (7)$$

where  $R$  is the universe gas coefficient;  $T$  is temperature; and  $C$  is the integration constant.

$\Delta\Omega$  is adopted to estimate the required work to reach adsorption equilibrium (Ridha and Webley, 2010).  $\Delta G$  is utilized to determine the spontaneity of sorption process.  $\Omega$  and  $\Delta G$  can be calculated by Eq. (8) and Eq. (9), respectively (Du et al., 2020b).

$$\Delta\Omega = -RT \int_0^P \frac{n}{P} dP \quad (8)$$

$$\Delta G = \frac{\Delta\Omega}{n} = -\frac{RT \int_0^P \frac{n}{P} dP}{n} \quad (9)$$

$\Delta S$  is useful to understand the variation in the disorderliness of adsorbate-adsorbent systems, which can be gained by Eq. (10) and Eq. (11) (Song et al., 2017).

$$\frac{\Delta S}{R} = \frac{\Delta h}{RT} - \frac{\mu}{RT} - \frac{\Delta\Omega}{nRT} \quad (10)$$

$$\Delta h = \frac{1}{n} \int_0^n Q_{st} dn \quad (11)$$

where  $\Delta h$  is the molar enthalpy of adsorption; and  $\mu$  is the chemical potential of the adsorbed gas.

## 5. Results and discussion

### 5.1. Pore structure of kaolinite clay

#### 5.1.1. Mesopore and macropore morphology of kaolinite clay

The  $N_2$  adsorption and desorption isothermal curves at 77 K are plotted in Fig. 1(a), and the pore size distribution (PSD) analyzed by  $N_2$  adsorption is described in Fig. 1(b). It is clear that when the relative pressure is high, adsorption isotherm and desorption isotherm do not coincide. The hysteresis loop given in Fig. 1(a) belongs to type H3, illustrating that kaolinite clay contains a large amount of mesopores and these mesopores are slit-shaped (Hwang and Pini, 2019). The slit-shaped mesopores are mainly formed by the particles stacking of platy mineral. In addition, as plotted in Fig. 1(b), kaolinite clay has a continuous PSD ranging from 1.5 nm to 38 nm.

Table 1 reports the pore structure parameters of kaolinite clay and shale obtained from  $N_2$  adsorption. Clearly, kaolinite clay does not have macropore, and the proportion of mesopore volume to total pore volume ( $V_{mes}/V_t$ ) is up to 90.00%. Accordingly, the BET specific surface area ( $S_{BET}$ ) and  $V_t$  of kaolinite clay are mainly contributed by mesopore.  $S_{BET}$  and  $V_t$  for shale are both higher than those for kaolinite clay. The higher  $S_{BET}$  and  $V_t$  are beneficial to the adsorption of fluid on shale. Meanwhile, unlike kaolinite clay, shale also has a certain amount of macropores. These macropores can offer more flow paths and facilitate the fluid movement. Therefore, fluid flow on actual shale reservoirs is easier than that on kaolinite clay.

#### 5.1.2. Micropore morphology of kaolinite clay

The measured adsorption isotherm of  $CO_2$  at 273.15 K is described in Fig. 2(a), and the PSD of micropore of kaolinite clay is presented in Fig. 2(b). As given in Fig. 2(b), the PSD of micropore of kaolinite clay is not continuous. The micropore of kaolinite clay is concentrated at 0.68 nm, 0.75 nm and 0.81 nm.

The comparison of micropore structure of kaolinite clay and shale is recorded in Table 2. The specific surface area ( $S_{CO_2}$ ) and volume ( $V_{CO_2}$ ) of micropore of kaolinite clay

obtained by the adsorption of  $CO_2$  are  $1.85 \text{ m}^2/\text{g}$  and  $0.00077 \text{ cm}^3/\text{g}$ , respectively.  $S_{CO_2}$  and  $V_{CO_2}$  for kaolinite clay are significantly lower than  $S_{BET}$  and  $V_t$  for kaolinite clay, respectively. Mesopore of kaolinite clay are more developed than micropore, and the studied kaolinite clay is mainly mesoporous material. As reported in Table 2,  $S_{CO_2}$  and  $V_{CO_2}$  for shale are both higher than those for kaolinite clay, indicating that shale has more developed micropore structure than kaolinite clay. With pore size decreases, the interaction energies on multiple surfaces superpose, leading to the noticeable improvement of attraction (Heller and Zoback, 2014). Consequently, micropore is more favorable for gas adsorption, and shale with well-developed micropore structure has greater adsorption capacity than kaolinite clay. In addition to clay minerals, shale also contains a certain amount of organic matter. The organic matter is responsible for the more developed micropore structure of shale.

### 5.2. Adsorption behaviors of $CH_4$ , $N_2$ and $CO_2$ in kaolinite clay

The obtained isothermal sorption curves of  $CO_2$ ,  $N_2$  and  $CH_4$  on kaolinite clay are displayed in Fig. 3(a), 3(b) and 3(c), respectively. Obviously, as the equilibrium pressure enhances, the uptakes for three gases all improve, suggesting that high pressure promotes  $CO_2$  storage and the accumulation of  $CH_4$ -in-place. Raising equilibrium pressure can give adsorbate molecules greater opportunity to collide with matrix surface, resulting in more adsorbate molecules to be retained in the adsorbed phase. Meanwhile, Jin and Fioozabadi (2014) found that  $CH_4$  and  $CO_2$  can also be trapped in the middle of bigger pores with increasing pressure when the micropores are occupied by previously injected  $CH_4$  and  $CO_2$ . As a result, high pressure can increase the uptakes of three gases on kaolinite clay.

From Fig. 3, it can be found that the uptakes of three gases all decrease monotonically with temperature. A higher experiment temperature indicates the larger average kinetic energy of adsorbate molecules (Tang et al., 2015). With improving temperature, the injected adsorbate molecules have the adequate energy to overcome the electrostatic force and van der Waals

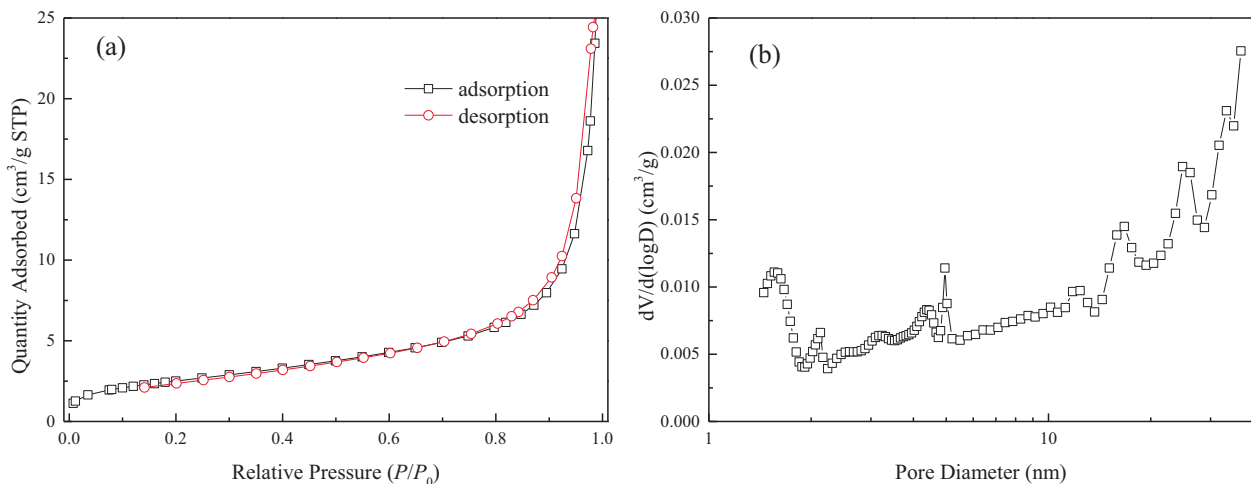


Fig. 1 Low-pressure  $N_2$  adsorption and desorption isotherms (a) and pore size distribution (b).

**Table 1** Pore structure of kaolinite clay and shale obtained from N<sub>2</sub> adsorption measurement.

Material	$V_t$ (cm <sup>3</sup> /g)	$V_{mac}$ (cm <sup>3</sup> /g)	$V_{mes}$ (cm <sup>3</sup> /g)	$V_{mic}$ (cm <sup>3</sup> /g)	$V_{mac}/V_t$ (%)	$V_{mes}/V_t$ (%)	$V_{mic}/V_t$ (%)	$S_{BET}$ (m <sup>2</sup> /g)	Data
Kaolinite clay	0.0160	0	0.0144	0.0016	0	90.00	10.00	9.11	This study
Nanchuan shale	0.0349	0.0038	0.0302	0.0009	10.89	86.53	2.58	35.41	Gu et al., 2017
Longmaxi shale	0.0239	0.0034	0.0169	0.0036	14.23	70.71	15.06	26.87	Gu et al., 2017

Note:  $V_{mac}$  is the macropore volume;  $V_{mes}$  is the mesopore volume;  $V_{mic}$  is the micropore volume; and  $V_t$  is the total pore volume.

force and stay in the gaseous phase (Zhou et al., 2012). The negative relation of adsorption quantity and temperature suggests that CO<sub>2</sub>, N<sub>2</sub> and CH<sub>4</sub> adsorption on kaolinite clay is an exothermic process.

By comparing the sorption performances of CO<sub>2</sub>, N<sub>2</sub> and CH<sub>4</sub> on kaolinite clay, we can see that the shape of adsorption isotherm of N<sub>2</sub> is different from those of CO<sub>2</sub> and CH<sub>4</sub>. N<sub>2</sub> adsorption isotherm is linear, while the isotherms of CO<sub>2</sub> and CH<sub>4</sub> belong to Type I isotherm according to International Union of Pure and Applied Chemistry (IUPAC) classification. The shape of isothermal sorption curves of CO<sub>2</sub> and CH<sub>4</sub> on studied kaolinite clay is similar to the results of Heller and Zoback (2014) about the sorption of CH<sub>4</sub> and CO<sub>2</sub> on pure kaolinite sample. The difference in the isotherm shapes for three gases denotes that the interaction of N<sub>2</sub>-kaolinite is distinct from those of CO<sub>2</sub>-kaolinite and CH<sub>4</sub>-kaolinite. When equilibrium pressure is small, the isothermal sorption curves of CO<sub>2</sub> and CH<sub>4</sub> are steeper, and their sorption rates are faster. As the pressure enlarges, the sorption rates of CO<sub>2</sub> and CH<sub>4</sub> gradually decline. At the initial stage, the available micropores for CO<sub>2</sub> and CH<sub>4</sub> are very plentiful. Meanwhile, previous study has pointed out the sorption potential will become deeper with the pore size decreases (Broom and Thomas, 2013). Hence, the abundant micropores with deeper sorption potential give rise to the quicker sorption of CO<sub>2</sub> and CH<sub>4</sub> at the early phase. However, for N<sub>2</sub> adsorption on kaolinite clay, the sorption rate almost keeps constant over the whole pressure range. The linear relation of the uptake of N<sub>2</sub> with pressure manifests that N<sub>2</sub> adsorption quantity is smaller and the

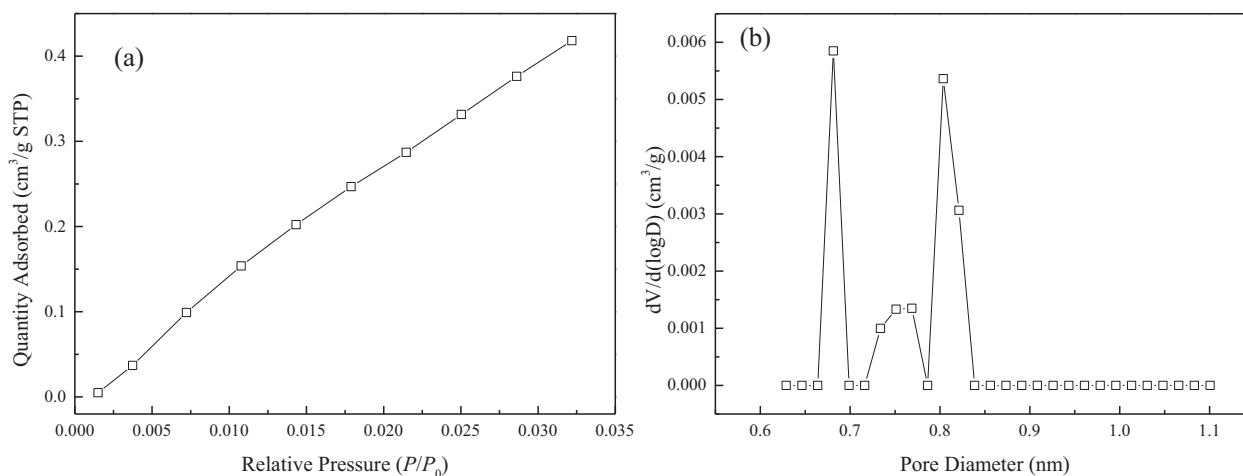
interaction of N<sub>2</sub>-kaolinite is weaker. This may be due to the pore size occupied by adsorbed N<sub>2</sub> is bigger than that occupied by adsorbed CO<sub>2</sub> and CH<sub>4</sub>. The bigger pore has the shallower adsorption potential, which leads to the slow and constant sorption rate of N<sub>2</sub>.

As depicted in Fig. 3, the order of the uptakes of three gases on kaolinite clay is as follows: CO<sub>2</sub> > CH<sub>4</sub> > N<sub>2</sub>, agreeing with the findings of Xiong et al. (2017). When researching the sorption of three gases on New Albany shale, Chareonsuppanimit et al. (2012) found that the ratio of adsorption capacities for N<sub>2</sub>, CH<sub>4</sub> and CO<sub>2</sub> is 1:3.2:9.3. The ratios of CO<sub>2</sub> adsorption amount ( $q_{CO_2}$ ) to N<sub>2</sub> adsorption amount ( $q_{N_2}$ ) and  $q_{CO_2}$  to CH<sub>4</sub> adsorption amount ( $q_{CH_4}$ ) on studied kaolinite clay are both lower than those on New Albany shale. The greater value of  $q_{CO_2}$  than  $q_{CH_4}$  on kaolinite clay supports the technical feasibility of applying CO<sub>2</sub>-ESGR project in kaolinite-rich shale reservoirs.

The difference in adsorption behaviors of CO<sub>2</sub>, N<sub>2</sub> and CH<sub>4</sub> on porous material is mainly due to the difference in physical

**Table 2** Micropore characterization results of kaolinite clay and shale.

Material	$V_{CO_2}$ (cm <sup>3</sup> /g)	$S_{CO_2}$ (m <sup>2</sup> /g)	Data
Kaolinite clay	0.00077	1.85	This study
Jiaoshiha shale	0.00370	9.32	Huo et al., 2017
Longmaxi shale	0.00964	9.20	Cheng et al., 2020

**Fig. 2** Adsorption isotherm of CO<sub>2</sub> (a) and micropore size distribution of kaolinite clay (b).

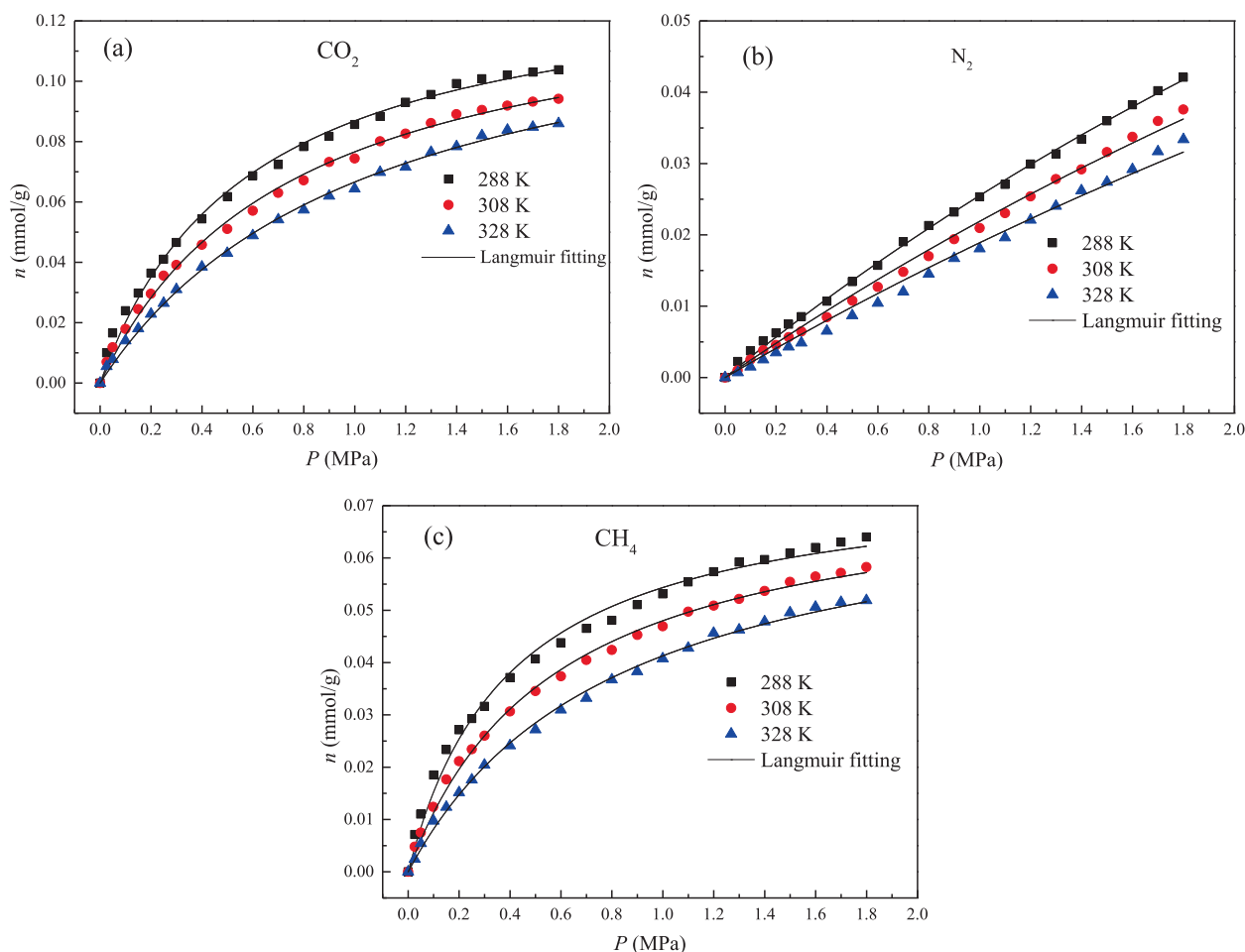


**Fig. 3** Isothermal adsorption curves at different temperatures: (a) CO<sub>2</sub>, (b) N<sub>2</sub> and (c) CH<sub>4</sub>.

characteristics of three gases, e.g., shape, polarity, kinetic diameter, dipole moment and quadrupole moment (Charriere et al., 2010). Table 3 summarizes the physical characteristics of CO<sub>2</sub>, N<sub>2</sub> and CH<sub>4</sub>. The linear shape and smaller kinetic diameter promote CO<sub>2</sub> to enter into more confined micropore, while these ultramicropores are only partly accessible to CH<sub>4</sub> owing to the molecule sieve effect. The research results of Liu et al. (2013) show that the available pore space for CH<sub>4</sub> adsorption within the organic matter is 40% smaller than that for the adsorption of CO<sub>2</sub>. Meanwhile, the boiling point of CH<sub>4</sub> is lower than that of CO<sub>2</sub>, which means that adsorbed CH<sub>4</sub> is easier to escape from the matrix by “evaporation” (Ettinger et al., 1966). Furthermore, CO<sub>2</sub> molecule possesses a permanent quadrupole moment, while CH<sub>4</sub> molecule is charge neutral. The quadrupole moment enhances the

interaction of CO<sub>2</sub>-kaolinite, bringing about the stronger adsorbed layer for CO<sub>2</sub> as confirmed by Jin and Firoozabadi (2014). Thereby, the studied kaolinite clay preferentially adsorbs CO<sub>2</sub> over CH<sub>4</sub>. The smaller adsorption quantity of N<sub>2</sub> than CH<sub>4</sub> on kaolinite clay is mainly attributed to the lower polarizability of N<sub>2</sub> molecule, which leads to the weaker interaction between N<sub>2</sub> and kaolinite clay.

Fig. 3 presents the matching results of the sorption isotherms using Langmuir model, and the corresponding fitting parameters in Langmuir model are detailed in Table 4. It is evident that the simulated data are consistent with the experimental results. The consistency between experimental data and modeling results over a broad pressure and temperature range implies the excellent applicability of Langmuir model to simulate three gases adsorption on kaolinite clay.

**Table 3** Physical characteristics of CO<sub>2</sub>, N<sub>2</sub> and CH<sub>4</sub>.

Gas	Shape	Boiling point (K)	Kinetic diameter (nm)	Polarizability (10 <sup>-24</sup> cm <sup>3</sup> )	Dipole moment (10 <sup>-18</sup> esu cm)	Quadrupole moment (10 <sup>-26</sup> esu cm <sup>2</sup> )
CO <sub>2</sub>	linear	194.65	0.330	2.65	0	4.30
CH <sub>4</sub>	tetrahedral	111.65	0.380	2.60	0	0
N <sub>2</sub>	linear	77.30	0.364	1.76	0	1.52

**Table 4** Langmuir fitting parameters of three gases on kaolinite clay.

Gas	$T$ (K)	$b$ (MPa <sup>-1</sup> )	$n_m$ (mmol/g)	ARE (%)	$R^2$
CO <sub>2</sub>	288	1.7070	0.1479	5.7993	0.9956
	308	1.3320	0.1310	5.7394	0.9966
	328	0.9221	0.1298	6.7149	0.9980
CH <sub>4</sub>	288	2.5078	0.0760	6.1598	0.9918
	308	1.7616	0.0753	4.8197	0.9967
	328	1.2197	0.0752	3.6734	0.9978
N <sub>2</sub>	288	0.1437	0.2031	5.4168	0.9987
	308	0.1234	0.1995	5.4650	0.9963
	328	0.1056	0.1975	9.9870	0.9918

### 5.3. Separation coefficients of CH<sub>4</sub>, N<sub>2</sub> and CO<sub>2</sub> in kaolinite clay

The calculated separation coefficients of CO<sub>2</sub> over CH<sub>4</sub> ( $\alpha_{\text{CO}_2/\text{CH}_4}$ ), CO<sub>2</sub> over N<sub>2</sub> ( $\alpha_{\text{CO}_2/\text{N}_2}$ ) and CH<sub>4</sub> over N<sub>2</sub> ( $\alpha_{\text{CH}_4/\text{N}_2}$ ) are recorded in Table 5. The values of  $\alpha_{\text{CO}_2/\text{CH}_4}$  are all bigger than one, demonstrating that the adsorbed CH<sub>4</sub> can be directly displaced by injected CO<sub>2</sub> on kaolinite clay. As listed in Table 5, the order of separation coefficients on kaolinite clay is as follows:  $\alpha_{\text{CO}_2/\text{N}_2} > \alpha_{\text{CH}_4/\text{N}_2} > \alpha_{\text{CO}_2/\text{CH}_4}$ . As the outstanding adsorption materials, clay minerals have been widely used for gas separation (Broom and Thomas, 2013). For CH<sub>4</sub> enrichment from extracted coalbed gas, whose main components are CH<sub>4</sub> and N<sub>2</sub>, addition of kaolinite clay to modify the adsorption materials can be considered. The values of  $\alpha_{\text{CO}_2/\text{CH}_4}$ ,  $\alpha_{\text{CO}_2/\text{N}_2}$  and  $\alpha_{\text{CH}_4/\text{N}_2}$  all exhibit a decreasing trend with temperature. Low temperature not only increases the uptake but also improves the separation efficiency. The negative relationship of  $\alpha_{\text{CO}_2/\text{CH}_4}$  with temperature has also been found on other adsorbents (Liu et al., 2018). Liu et al. (2018) thought that the induced desorption of adsorbate from matrix surface is the main reason for the decrease in  $\alpha_{\text{CO}_2/\text{CH}_4}$  at high temperature. Meanwhile, in the previous study about CO<sub>2</sub> and CH<sub>4</sub> competitive adsorption on kerogen,  $\alpha_{\text{CO}_2/\text{CH}_4}$  also continuously declines with pressure (Anh et al., 2018). Therefore, the shallow shale reservoirs with lower temperature and pressure condition boost the replacement of adsorbed CH<sub>4</sub> by CO<sub>2</sub>, agreeing with the findings of Wang et al (2018).

The values of  $\alpha_{\text{CO}_2/\text{CH}_4}$  on shale are also shown in Table 5. It can be found from Table 5 that  $\alpha_{\text{CO}_2/\text{CH}_4}$  values on shale are bigger than those on kaolinite clay, elucidating that the actual shale formation is more suitable for the extraction of CH<sub>4</sub> by

CO<sub>2</sub> injection. The findings of Wang and Huang (2019) pointed out  $\alpha_{\text{CO}_2/\text{CH}_4}$  reduces as the pore size enlarges. As discussed in Section 5.1, shale has a more developed micropore structure. Accordingly, even though increasing kaolinite clay content can improve the adsorption ability of shale, it damages the displacement efficiency of CO<sub>2</sub> on shale. Hence, to select the target reservoir for implementation of CO<sub>2</sub>-ESGR project, the content of kaolinite clay in shale sediment needs to be paid more attention.

### 5.4. Adsorption affinities of CH<sub>4</sub>, N<sub>2</sub> and CO<sub>2</sub> in kaolinite clay

The gained  $K_H$  of CH<sub>4</sub>, N<sub>2</sub> and CO<sub>2</sub> in kaolinite clay are listed in Table 6. CO<sub>2</sub> has a largest  $K_H$ , while the  $K_H$  value of N<sub>2</sub> is the smallest. The adsorption affinity of CO<sub>2</sub> on kaolinite clay is biggest, and N<sub>2</sub> has a lowest affinity. For the adsorbate-adsorbent pair, the interaction strength depends on dipole moment-field gradient interaction energy, quadrupole moment-field gradient and induction energy (Deng et al., 2012). As given in Table 3, the highest quadrupole moment and polarizability make the strongest interaction of CO<sub>2</sub>-kaolinite and the largest  $K_H$  for CO<sub>2</sub>. Although N<sub>2</sub> molecule has a quadrupole moment, CH<sub>4</sub> polarizability is higher. The combined effect results in the larger  $K_H$  for CH<sub>4</sub> than N<sub>2</sub>. In addition, temperature has a negative impact on  $K_H$  for three gases, revealing that increasing temperature can decrease the adsorption affinity.

The comparison of  $K_H$  for CH<sub>4</sub> and CO<sub>2</sub> on kaolinite clay and shale is elucidated in Table 6. The difference in  $K_H$  for CH<sub>4</sub> and CO<sub>2</sub> on Youyang shale and Weiyuan shale is more apparent than that on kaolinite clay. Because  $K_H$  has a positive

**Table 5** Separation coefficients on kaolinite clay and shale.

Material	$P$ (MPa)	$T$ (K)	$\alpha_{\text{CO}_2/\text{CH}_4}$	$\alpha_{\text{CO}_2/\text{N}_2}$	$\alpha_{\text{CH}_4/\text{N}_2}$	Data
Kaolinite clay	0–1.80	288	1.67	8.65	6.53	This study
	0–1.80	308	1.65	7.08	5.39	
	0–1.80	328	1.61	5.74	4.40	
Wufeng shale	0–1.80	278–318	4.98–7.04			Gu et al., 2017
Longmaxi shale	0–1.80	278–318	2.87–4.33			
Nanchuan shale	0–1.80	278–318	3.82–6.63			
Fuling shale	0–1.80	278–318	3.29–4.77			
Marcellus shale	0–27.50	313	4.76			Pei et al., 2015
Eagle Ford shale	0–41.30	313	4.42			

**Table 6** Henry's coefficients on kaolinite clay and shale.

Material	Gas	$T$ (K)	$K_H$	Gas	$T$ (K)	$K_H$	Gas	$T$ (K)	$K_H$	Data
Kaolinite clay		288	0.39		288	0.19		288	0.05	This study
	CO <sub>2</sub>	308	0.26	CH <sub>4</sub>	308	0.18	N <sub>2</sub>	308	0.03	
		328	0.16		328	0.12		328	0.01	
Youyang shale		278	1.13		278	0.12				Duan, 2017
	CO <sub>2</sub>	298	0.65	CH <sub>4</sub>	298	0.11				
		318	0.44		318	0.07				
Weiyuan shale		278	0.86		278	0.11				Duan, 2017
	CO <sub>2</sub>	298	0.54	CH <sub>4</sub>	298	0.09				
		318	0.32		318	0.07				

Note: the unit of  $K_H$  is mmol/g/MPa.

correlation with adsorption quantity, the difference in the uptakes of CH<sub>4</sub> and CO<sub>2</sub> on kaolinite clay is smaller. This smaller difference in the uptakes of CH<sub>4</sub> and CO<sub>2</sub> on kaolinite clay is not conducive to the enlargement of  $\alpha_{\text{CO}_2/\text{CH}_4}$ . Therefore,  $\alpha_{\text{CO}_2/\text{CH}_4}$  on shale is greater than that on kaolinite clay.

From Table 6, we can find that  $K_H$  values of CO<sub>2</sub> on two shale samples are both higher than that on kaolinite clay, which reflects that the adsorption affinity and adsorption capacity of CO<sub>2</sub> are larger on shale. For example, the uptake of CO<sub>2</sub> on Youyang shale is 0.17 mmol/g under 298 K and 1.80 MPa, while the uptake of CO<sub>2</sub> on kaolinite clay under a lower temperature of 288 K and 1.80 MPa is only 0.10 mmol/g. In addition,  $K_H$  values of CH<sub>4</sub> on kaolinite clay are slightly bigger than those on shale. Therefore, the uptakes of CH<sub>4</sub> on kaolinite clay and shale are almost equivalent.

### 5.5. Thermodynamics analysis of CH<sub>4</sub>, N<sub>2</sub> and CO<sub>2</sub> in kaolinite clay

#### 5.5.1. Surface potentials of CH<sub>4</sub>, N<sub>2</sub> and CO<sub>2</sub> in kaolinite clay

Surface potential  $\Delta\Omega$  corresponds to the needed minimum work to load adsorption material to reach a specific level (Mofarahi and Bakhtyari, 2015). Fig. 4 presents the gained  $\Delta\Omega$  of three gases in kaolinite clay. The  $\Delta\Omega$  values of three gases under experimental temperature and pressure are all negative. The absolute values of  $\Delta\Omega$  versus equilibrium pressure show a rapid increase upon further filling of adsorbate molecules into pore space. Under higher pressure (loading) condition, the more isothermal work is needed to load additional adsorbate molecules into the pore structure than at the preliminary stage (Ridha and Webley, 2010). The enhancement of isothermal work for adsorbate molecules with pressure is owing to the screened active sorption sites of porous material. As depicted in Fig. 4,  $\Delta\Omega$  for three gases are close to zero when the equilibrium pressure approaches zero. On the basis of the definition of  $\Delta\Omega$  proposed by Van Ness, the specific chemical potential of porous media in contact with molecules is becoming equal to the specific potential of porous media without contact with molecules at lower loading condition (Van, 1969). Thereby, reducing pressure causes  $\Delta\Omega$  to approach zero.

It is clear that the absolute values of  $\Delta\Omega$  for three gases display a noticeable reduction upon the temperature improvement from 288 K to 328 K. Previous study has shown that

the less adsorption quantity brings about the lower (less negative) surface potential (Du et al., 2020b). Thus, adsorption amount and surface potential both reduce as the temperature increases. This is because the less adsorbate molecules are required to fill into cavity pore under higher temperature.

At the same condition, CO<sub>2</sub> has the biggest absolute value of  $\Delta\Omega$ , while N<sub>2</sub> possesses the smallest absolute value of  $\Delta\Omega$ . The smallest uptake of N<sub>2</sub> on kaolinite clay results in the least isothermal work and the lowest  $\Delta\Omega$ . The increase rates of  $\Delta\Omega$  for CO<sub>2</sub> and CH<sub>4</sub> are larger at the early stage, and then they reduce gradually with pressure. However, the increase rate of  $\Delta\Omega$  for N<sub>2</sub> keeps the same over the whole pressure range. The variation trends of  $\Delta\Omega$  with pressure are accordant with the change trends of the uptakes of three gases with pressure.

#### 5.5.2. Changes of Gibbs free energy of CH<sub>4</sub>, N<sub>2</sub> and CO<sub>2</sub> in kaolinite clay

When temperature and pressure keep constant, the increment of free energy per unit surface area is called Gibbs free energy (Zhou et al., 2011). Gibbs free energy is caused by the asymmetric force field of atoms (molecules or ions) on the material surface (Nie et al., 2000). When the surface of porous material is formed, the force acting on the surface atoms is unbalanced, and the surface atoms are affected by the attraction which points vertically to the interior of solid. Therefore, the surface atoms tend to move towards the interior of solid, which makes the surface atoms to obtain an additional energy, namely, Gibbs free energy. Accordingly, the change of Gibbs free energy  $\Delta G$  is a critical parameter to measure the spontaneity of adsorption system. Fig. 5 describes  $\Delta G$  of three gases in kaolinite clay.  $\Delta G$  values of three gases are all negative, which indicates that gas adsorption in kaolinite clay is spontaneous process.

As the pressure rises, the absolute value of  $\Delta G$  enhances, showing that increasing pressure improves the spontaneity of sorption. As a result, there is a monotonous enhancement of the uptake with pressure. Injection of N<sub>2</sub> into shale reservoir can cause CH<sub>4</sub> desorption by reducing CH<sub>4</sub> partial pressure and lowering CH<sub>4</sub> adsorption spontaneity. The technology of N<sub>2</sub>-ESGR is also feasible to drive CH<sub>4</sub> exploitation. Moreover, the influence of pressure on  $\Delta G$  of CH<sub>4</sub> and CO<sub>2</sub> is more evident than that of N<sub>2</sub>. For N<sub>2</sub> adsorption on kaolinite clay, improving temperature decreases the spontaneity of adsorption. For the sorption of CH<sub>4</sub> and CO<sub>2</sub>, the relation of  $\Delta G$  with temperature is complicated. At the pressure larger than

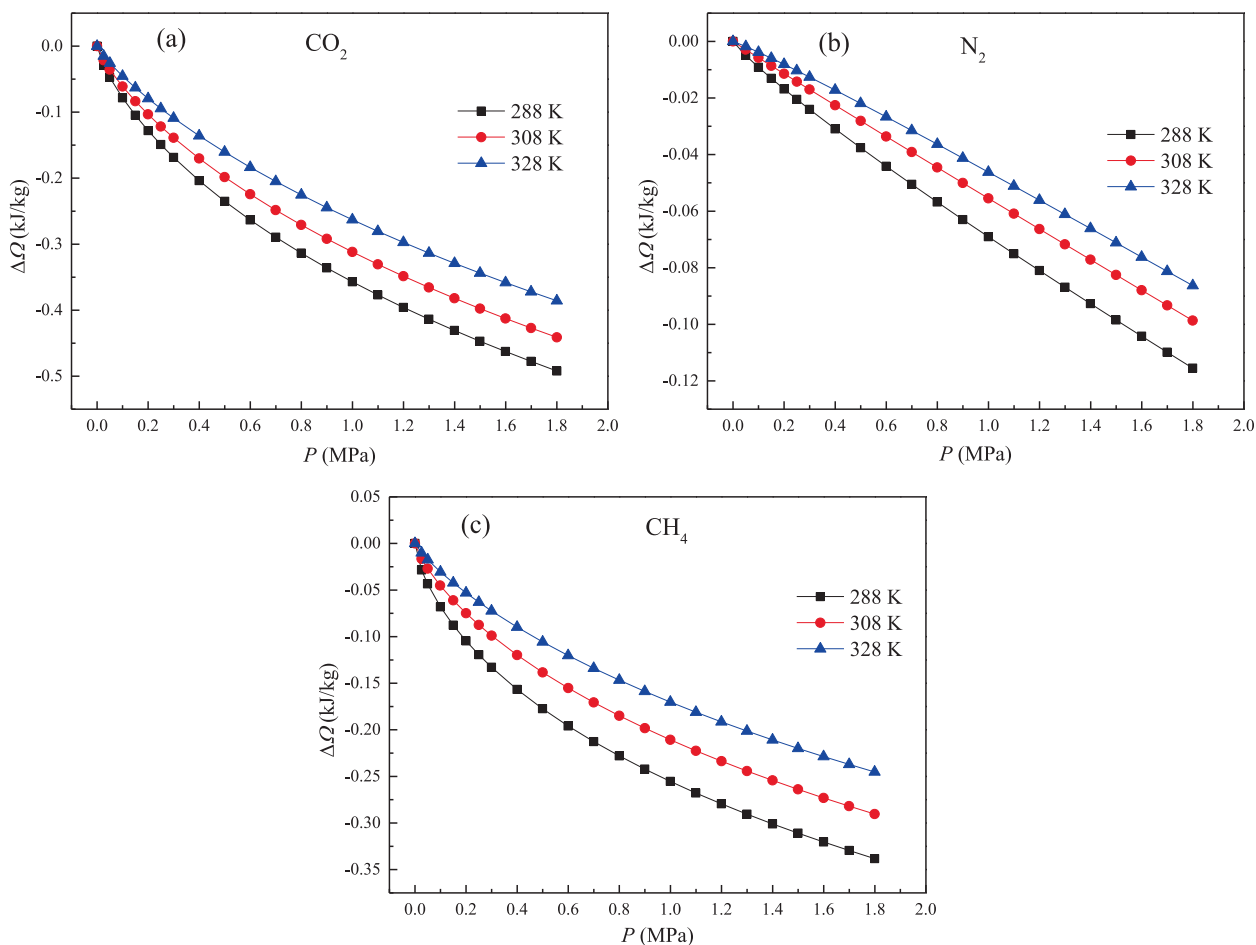


Fig. 4 Surface potentials at different temperatures: (a) CO<sub>2</sub>, (b) N<sub>2</sub> and (c) CH<sub>4</sub>

0.10 MPa, low temperature helps to gain higher  $\Delta G$  of CO<sub>2</sub>. When pressure is higher than 0.50 MPa, low temperature corresponds to the higher  $\Delta G$  of CH<sub>4</sub>. Therefore, only under the condition of high pressure, low temperature facilitates the spontaneity of adsorption of CO<sub>2</sub> and CH<sub>4</sub> in kaolinite clay.

As given in Fig. 5, the absolute value of  $\Delta G$  of CO<sub>2</sub> is the biggest, while N<sub>2</sub> has the smallest absolute value of  $\Delta G$ . Consequently, CO<sub>2</sub> adsorption on kaolinite clay has the highest spontaneity, and the spontaneity degree of N<sub>2</sub> adsorption on kaolinite clay is the lowest. According to the minimum energy principle, the lower the system energy is, the more stable the system is (Zhou et al., 2011). The matrix surface always tries to adsorb other substances around to reduce the surface free energy. The larger change of surface free energy gives the adsorption material a greater motivation to reduce energy by adsorbing gas. Therefore, CO<sub>2</sub> with biggest  $\Delta G$  has the largest uptake on kaolinite clay, while the adsorption of N<sub>2</sub> on kaolinite clay is the most difficult.

The change of surface free energy is not only related to the spontaneity of adsorption, but also to the matrix deformation. As pointed out by Nie et al. (2000), the larger change of surface free energy can lead to the greater deformation and the easier fracture of coal body. For the selection of site for CO<sub>2</sub> geological sequestration, one of most significant factors is the long-term stability of CO<sub>2</sub> storage (Huang et al., 2018). To increase the safety of CO<sub>2</sub> sequestration into deep subsur-

face and reduce the risk in CO<sub>2</sub> leakage into surrounding strata, more efforts should be focused on the deformation and the change of strength of shale after CO<sub>2</sub> adsorption.

### 5.5.3. Isothermic heats of adsorption of CH<sub>4</sub>, N<sub>2</sub> and CO<sub>2</sub> in kaolinite clay

Isothermic heat of adsorption  $Q_{st}$  indicates adsorption heat effect and is one of the critical variables for the design of adsorptive separation process. Fig. 6 depicts the acquired  $Q_{st}$  of three gases versus loading in kaolinite clay. The enthalpy change  $\Delta H$  ( $-Q_{st}$ ) values for three gases are negative, which confirms that the adsorption of three gases in kaolinite clay is exothermic process. All of  $Q_{st}$  values are smaller than 40 kJ/mol, validating that the adsorption of three gases in kaolinite clay is physisorption.

With the loading increases,  $Q_{st}$  for three gases all show a monotonous downward trend. If the adsorption material surface is energetically homogeneous,  $Q_{st}$  is not relevant to the loading, while  $Q_{st}$  changes with loading when the adsorption material surface is energetically heterogeneous (Chakraborty et al., 2006; Sircar, 1991). The decrease in  $Q_{st}$  with loading proves the heterogeneous surface of kaolinite clay. During the adsorption process,  $Q_{st}$  value is affected by the interaction energy of adsorbate-adsorbate and adsorbate-adsorbent pairs. At the preliminary stage of adsorption, lots of active adsorption sites are available, and the adsorbates are directly

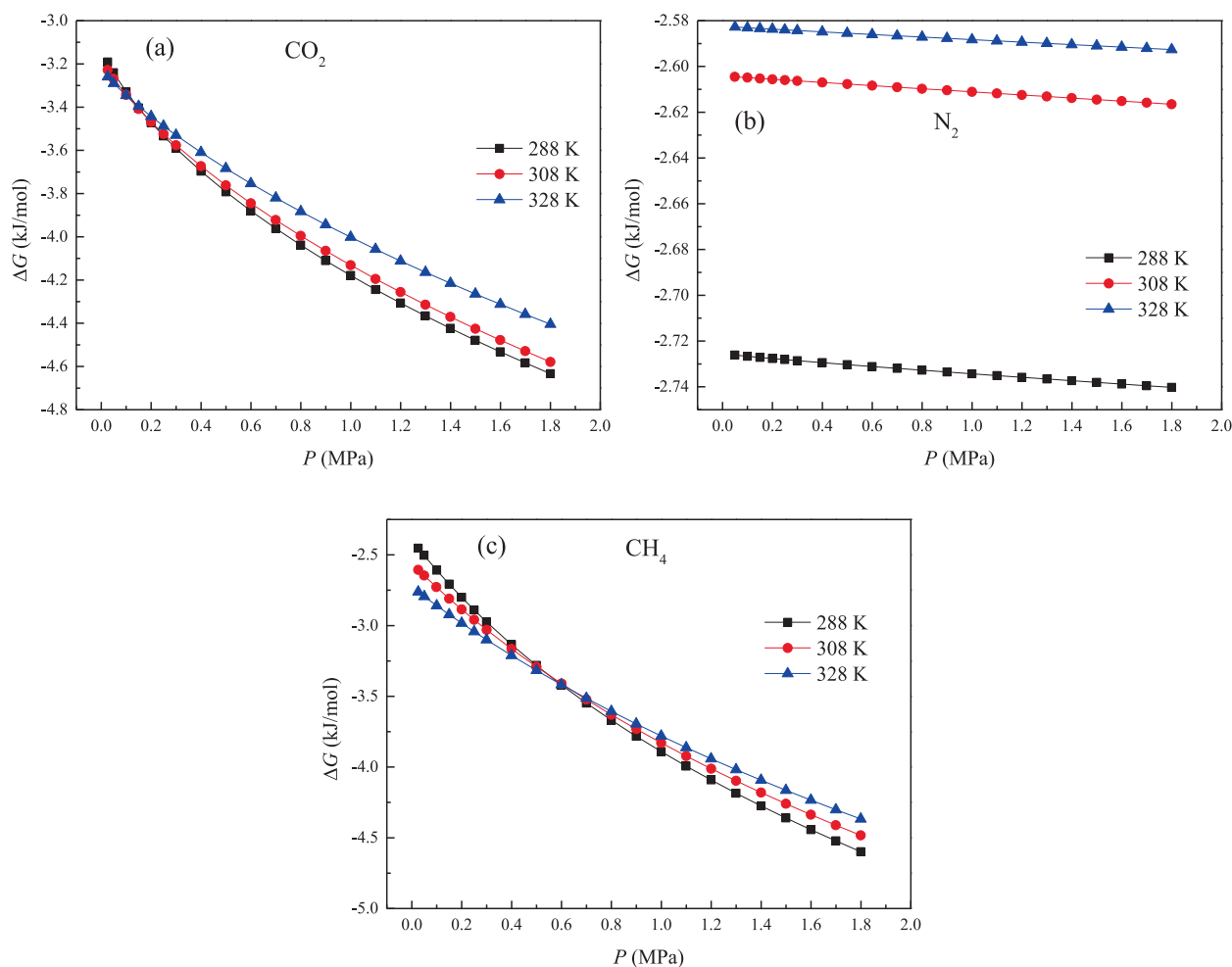


**Fig. 5** Changes of Gibbs free energy at different temperatures: (a) CO<sub>2</sub>, (b) N<sub>2</sub> and (c) CH<sub>4</sub>.

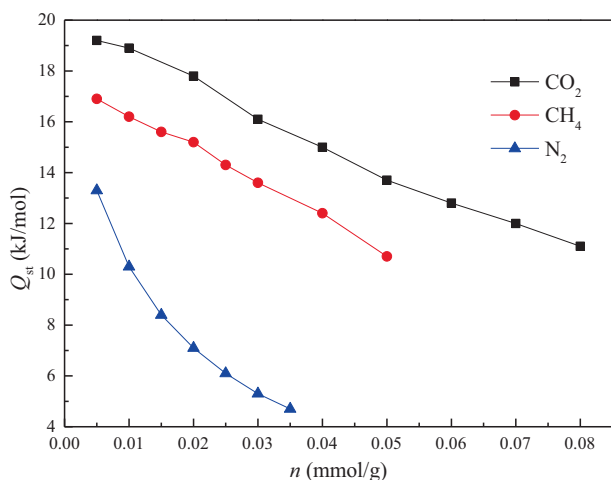


**Fig. 6** Isothermic heats of adsorption for three gases in kaolinite clay.

adsorbed on the preferential adsorption sites, causing the stronger force between adsorbate and adsorbent and the weaker lateral interaction between adsorbate molecules. As

the loading increases, more and more pore space is occupied, and the interaction energy of adsorbate-adsorbent is lower than adsorbate-adsorbate interaction energy. Thus,  $Q_{st}$  declines with improving loading.

Clearly, CO<sub>2</sub> has the largest  $Q_{st}$ , and  $Q_{st}$  value of N<sub>2</sub> is the smallest. The biggest  $Q_{st}$  indicates that the interaction of CO<sub>2</sub>-kaolinite is the strongest. Accordingly, N<sub>2</sub> with the lowest  $Q_{st}$  has the weakest interaction with kaolinite. The quadrupole moment strengthens the interaction of CO<sub>2</sub> with kaolinite, and hence CO<sub>2</sub> adsorption gives off more heat. Meanwhile,  $Q_{st}$  enhances constantly until the diameter ratio of the pore to the molecular approaches one, and increasing pore curvature has a positive effect on  $Q_{st}$  (Keffer et al., 1996). Because CO<sub>2</sub> can migrate into smaller pores, more heat is released for CO<sub>2</sub> adsorption. The reduction rate of  $Q_{st}$  with loading for N<sub>2</sub> is the fastest. The rapid decrease in  $Q_{st}$  illustrates the weaker intermolecular force between N<sub>2</sub> molecules at the late stage of adsorption.

#### 5.5.4. Entropy losses of CH<sub>4</sub>, N<sub>2</sub> and CO<sub>2</sub> in kaolinite clay

Entropy loss  $\Delta S$  is defined as the change from the entropy of a clean porous material and adsorbates in the perfect-gas state to that of the adsorption system containing a porous material with adsorbed molecules inside its pore (Myers, 2004). Infor-

mation about  $\Delta S$  during the adsorption process is conducive to comprehending the packing pattern and the confined mobility of adsorbed adsorbates.

The results of  $\Delta S$  of three gases are detailed in Fig. 7. From Fig. 7, it can be seen that  $\Delta S$  values are all negative, indicating that gas adsorption in kaolinite clay is from an unrestricted stage to a restricted stage. As reported by Zhou et al. (2012), adsorption always implies the formation of a more orderly rearrangement on matrix surface and the loss of the degree of freedom of molecules. Within the micropore, the value of translational entropy is bigger than that of rotational entropy, and the majority of entropy loss is contributed by the loss of translational degree during sorption process (Myers, 2004). Therefore, the translation of molecules is more limited in the micropore.

As the loading increases, the absolute values of  $\Delta S$  for three gases decline. Larger adsorption loading causes the lower (less negative)  $\Delta S$ . When the available pore is gradually occupied by adsorbate molecules, the disorderliness degree of investigated adsorption system increases. Therefore, higher adsorption loading condition is unfavorable for the efficient packing. At the early phase, molecules are adsorbed in the smaller pores, and the adsorbed molecules are more confined. With the increase in loading, the majority of injected molecules are retained in the bigger pores. In these large pores, the movement of adsorbed molecule is not effectively limited, bringing about the lower  $\Delta S$ . In addition, under different temperatures, the curves of  $\Delta S$  basically coincide. Therefore, temperature has a negligible influence on  $\Delta S$ , which is in accordance with the report of Duan et al. (2016) about CH<sub>4</sub> and CO<sub>2</sub> adsorption on shale.

It should be noted that  $\Delta S$  of N<sub>2</sub> is the lowest, while CO<sub>2</sub> has the highest  $\Delta S$ . Myers (2004) discovered that the adsorbent with smaller pores has bigger absolute values of entropy change. Due to the more restricted pore for CO<sub>2</sub> adsorption, the movement of adsorbed CO<sub>2</sub> is more difficult. Meanwhile, the higher quadrupole moment and polarizability enhance the interaction of CO<sub>2</sub>-kaolinite, giving rise to the more efficient adsorbate packing by producing the structured fluid. Therefore,  $\Delta S$  values of CO<sub>2</sub> are higher than those of N<sub>2</sub> and CH<sub>4</sub>. The highest  $\Delta S$  reveals that adsorbed CO<sub>2</sub> molecules

form a most ordered rearrangement. The smaller  $\Delta S$  for N<sub>2</sub> than CH<sub>4</sub> is because of the lower polarizability of N<sub>2</sub>, which induces the weaker interaction between electrostatic-field gradients and N<sub>2</sub> molecules. Furthermore, the decrease of  $\Delta S$  for N<sub>2</sub> with loading is more rapid than those for CO<sub>2</sub> and CH<sub>4</sub>. The quick reduction of  $\Delta S$  for N<sub>2</sub> elucidates the weaker interaction strength of N<sub>2</sub>-kaolinite and the lower orderliness of adsorbed N<sub>2</sub> on kaolinite surface.

## 6. Conclusions

In this paper, the adsorption experiments of CO<sub>2</sub>, N<sub>2</sub> and CH<sub>4</sub> at 288 K, 308 K and 328 K on kaolinite clay were conducted. The thermodynamics analysis of CO<sub>2</sub>, N<sub>2</sub> and CH<sub>4</sub> adsorption was performed to explain the adsorption behavior and understand the adsorption mechanism. The main conclusions are as following:

- (1) The values of  $\alpha_{\text{CO}_2/\text{CH}_4}$  are greater than one, confirming the feasibility of replacement of adsorbed CH<sub>4</sub> by CO<sub>2</sub> on kaolinite clay. The values of  $\alpha_{\text{CO}_2/\text{CH}_4}$ ,  $\alpha_{\text{CO}_2/\text{N}_2}$  and  $\alpha_{\text{CH}_4/\text{N}_2}$  all exhibit a decreasing trend with temperature. The shallow gas-bearing reservoir is beneficial for the enhanced CH<sub>4</sub> recovery by CO<sub>2</sub> injection.
- (2) The adsorption affinity for three gases on kaolinite clay is as follows: CO<sub>2</sub> > CH<sub>4</sub> > N<sub>2</sub>. CO<sub>2</sub> has a strongest interaction with kaolinite clay, while the interaction of N<sub>2</sub>-kaolinite is the lowest.
- (3) The spontaneity degree of CO<sub>2</sub> adsorption on kaolinite clay is the highest, while N<sub>2</sub> has the lowest adsorption spontaneity on kaolinite clay. Injecting N<sub>2</sub> into shale reservoir can cause CH<sub>4</sub> desorption by lowering the spontaneity of CH<sub>4</sub> adsorption. Adsorbed CO<sub>2</sub> molecules form a most ordered rearrangement on kaolinite surface.

## 7. Data availability

The data applied to support the results in this study are available from the corresponding author upon request.

## CRedit authorship contribution statement

**Xidong Du:** Writing – original draft. **Dongdong Pang:** Conceptualization, Supervision. **Yuan Zhao:** Data curation, Resources. **Zhenkun Hou:** Formal analysis, Project administration. **Hanglong Wang:** Investigation. **Yugang Cheng:** Methodology.

## Declaration of Competing Interest

The authors declare that they have no known competing financial interests or personal relationships that could have appeared to influence the work reported in this paper.

## Acknowledgments

This study was supported by Yunnan Fundamental Research Projects (Grant No. 202101BE070001-039), Yunnan Department of Education Science Research Fund Project (Grant No. 2022J0055), National Natural Science Foundation of China (Grant No. 51904049), China Postdoctoral Science Foundation (Grant No. 2021M693750), and Open Research

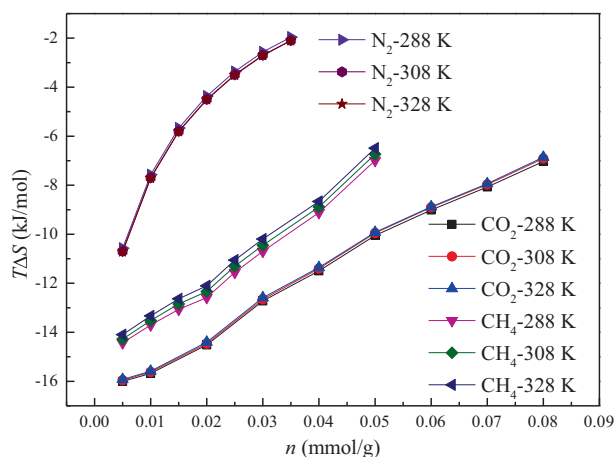


Fig. 7 Entropy losses for three gases at different temperatures.

Fund of Key Laboratory of Safety and High-efficiency Coal Mining, Ministry of Education, Anhui University of Science and Technology (Grant No. JYBSYS2020207).

## References

- Anh, Ho. T., Wang, Y.F., Xiong, Y.L., Criscenti, L.J., 2018. Differential retention and release of CO<sub>2</sub> and CH<sub>4</sub> in kerogen nanopores: implications for gas extraction and carbon sequestration. *Fuel* 220, 1–7.
- Broom, D.P., Thomas, K.M., 2013. Gas adsorption by nanoporous materials: future applications and experimental challenges. *Mrs Bull.* 38 (5), 412–421.
- Chakraborty, A., Saha, B.B., Koyama, S., 2006. On the thermodynamic modeling of the isosteric heat of adsorption and comparison with experiments. *Appl. Phys. Lett.* 89, 171901.
- Chareonsuppanimit, P., Mohammad, S.A., Robinson, J.R.L., Gasem, K.A.M., 2012. High-pressure adsorption of gases on shales: measurements and modeling. *Int. J. Coal Geol.* 95, 34–46.
- Charriere, D., Pokryszka, Z., Behra, P., 2010. Effect of pressure and temperature on diffusion of CO<sub>2</sub> and CH<sub>4</sub> into coal from the Lorraine basin (France). *Int. J. Coal Geol.* 81, 373–380.
- Cheng, Y.G., Zeng, M.R., Lu, Z.H., Du, X.D., Yin, H., Yang, L., 2020. Effects of supercritical CO<sub>2</sub> treatment temperatures on mineral composition, pore structure and functional groups of shale: implications for CO<sub>2</sub> sequestration. *Sustainability* 12, 3927.
- Deng, H., Yi, H.H., Tang, X.L., Yu, Q.F., Ning, P., Yang, L.P., 2012. Adsorption equilibrium for sulfur dioxide, nitric oxide, carbon dioxide, nitrogen on 13X and 5A zeolites. *Chem. Eng. J.* 188, 77–85.
- Du, X.D., Cheng, Y.G., Liu, Z.J., Hou, Z.K., Wu, T.F., Lei, R.D., Shu, C.X., 2020a. Study on the adsorption of CH<sub>4</sub>, CO<sub>2</sub> and various CH<sub>4</sub>/CO<sub>2</sub> mixture gases on shale. *Alex. Eng. J.* 59, 5165–5178.
- Du, X.D., Cheng, Y.G., Liu, Z.J., Yin, H., Wu, T.F., Huo, L., Shu, C. X., 2021a. CO<sub>2</sub> and CH<sub>4</sub> adsorption on different rank coals: A thermodynamics study of surface potential, Gibbs free energy change and entropy loss. *Fuel* 283, 118886.
- Du, X.D., Gu, M., Duan, S., Xian, X.F., 2017. Investigation of CO<sub>2</sub>-CH<sub>4</sub> displacement and transport in shale for enhanced shale gas recovery and CO<sub>2</sub> sequestration. *ASME J. Energy Resour. Technol.* 139, 012909.
- Du, X.D., Gu, M., Duan, S., Xian, X.F., 2018. The influence of CO<sub>2</sub> injection pressure on CO<sub>2</sub> dispersion and the mechanism of CO<sub>2</sub>-CH<sub>4</sub> displacement in shale. *ASME J. Energy Resour. Technol.* 140, 012907.
- Du, X.D., Gu, M., Hou, Z.K., Liu, Z.J., Wu, T.F., 2019a. Experimental study on the kinetics of adsorption of CO<sub>2</sub> and CH<sub>4</sub> in gas-bearing shale reservoirs. *Energy Fuel* 33, 12587–12600. <https://doi.org/10.1021/acs.energyfuels.9b03176>.
- Du, X.D., Gu, M., Liu, Z.J., Zhao, Y., Sun, F.L., Wu, T.F., 2019b. Enhanced shale gas recovery by the injections of CO<sub>2</sub>, N<sub>2</sub>, and CO<sub>2</sub>/N<sub>2</sub> mixture gases. *Energy Fuel* 33, 5091–5101.
- Du, X.D., Guang, W.F., Cheng, Y.G., Hou, Z.K., Liu, Z.J., Yin, H., Huo, L., Lei, R.D., Shu, C.X., 2020b. Thermodynamics analysis of the adsorption of CH<sub>4</sub> and CO<sub>2</sub> on montmorillonite. *Appl. Clay Sci.* 192, 105631.
- Du, X.D., Pang, D.D., Cheng, Y.G., Zhao, Y., Hou, Z.K., Liu, Z.J., Wu, T.F., Shu, C.X., 2021b. Adsorption of CH<sub>4</sub>, N<sub>2</sub>, CO<sub>2</sub>, and their mixture on montmorillonite with implications for enhanced hydrocarbon extraction by gas injection. *Appl. Clay Sci.* 210, 106160.
- Du, X.D., Wang, N., 2021. Investigation into adsorption equilibrium and thermodynamics for water vapor on montmorillonite clay. *AIChE J.* e17550 <https://doi.org/10.1002/aic.17550>.
- Duan, S., 2017. A thermodynamics study of CO<sub>2</sub> and CH<sub>4</sub> adsorption on Sichuan basin shales. Chongqing University, Chongqing, China.
- Duan, S., Gu, M., Du, X.D., Xian, X.F., 2016. Adsorption equilibrium of CO<sub>2</sub> and CH<sub>4</sub> and their mixture on Sichuan basin shale. *Energy Fuel* 30, 2248–2256.
- Ettinger, I., Eremin, I., Zimakov, B., Yanovskaya, M., 1966. Natural factors influencing coal sorption properties. I. Petrography and sorption properties of coals. *Fuel* 45, 267–275.
- Gu, M., Xian, X.F., Duan, S., Du, X.D., 2017. Influences of the composition and pore structure of a shale on its selective adsorption of CO<sub>2</sub> over CH<sub>4</sub>. *J. Nat. Gas Sci. Eng.* 46, 296–306.
- Hameed, K.S., Muthirulan, P., Sundaram, M.M., 2017. Adsorption of chromotrope dye onto activated carbons obtained from the seeds of various plants: equilibrium and kinetic studies. *Arab. J. Chem.* 10, S2225–S2233.
- Heller, R., Zoback, M., 2014. Adsorption of methane and carbon dioxide on gas shale and pure mineral samples. *J. Unconventional Oil Gas Resources* 8, 14–24.
- Huang, L., Ning, Z.F., Wang, Q., Zhang, W.T., Cheng, Z.L., Wu, X. J., Qin, H.B., 2018. Effect of organic type and moisture on CO<sub>2</sub>/CH<sub>4</sub> competitive adsorption in kerogen with implications for CO<sub>2</sub> sequestration and enhanced shale gas recovery. *Appl. Energy* 210, 28–43.
- Huo, P.L., Zhang, D.F., Yang, Z., Li, W., Zhang, J., Jia, S.Q., 2017. CO<sub>2</sub> geological sequestration: displacement behavior of shale gas methane by carbon dioxide injection. *Int. J. Greenh. Gas Con.* 66, 48–59.
- Hwang, J., Pini, R., 2019. Supercritical CO<sub>2</sub> and CH<sub>4</sub> uptake by illite-smectite clay minerals. *Environ. Sci. Technol.* 53, 11588–11596.
- Jessen, K., Tang, G.Q., Kovscek, A.R., 2008. Laboratory and simulation investigation of enhanced coalbed methane recovery by gas injection. *Transp. Porous Med.* 73, 141–159.
- Jin, Z.H., Firoozabadi, A., 2014. Effect of water on methane and carbon dioxide sorption in clay minerals by Monte Carlo simulations. *Fluid Phase Equilib.* 382, 10–20.
- Kamboh, M.A., Bhatti, A.A., Solangi, I.B., Sherazi, S.T.H., Memon, S., 2014. Adsorption of direct black-38 azo dye on *p-tert*-butylcalix [6]arene immobilized material. *Arab. J. Chem.* 7, 125–131.
- Kang, G.X., Zhang, B., Kang, T.H., Guo, J.Q., Zhao, G.F., 2020. Effect of pressure and temperature on CO<sub>2</sub>/CH<sub>4</sub> competitive adsorption on kaolinite by Monte Carlo simulations. *Materials* 13, 2851.
- Keffer, D., Davis, H.T., McCormick, A.V., 1996. The effect of nanopore shape on the structure and isotherms of adsorbed fluids. *Adsorption* 2, 9–21.
- Liu, F.Y., Ellett, K., Xiao, Y.T., Rupp, J.A., 2013. Assessing the feasibility of CO<sub>2</sub> storage in the New Albany shale (Devonian-Mississippian) with potential enhanced gas recovery using reservoir simulation. *Int. J. Greenh. Gas Con.* 17, 111–126.
- Liu, B., Qi, C., Mai, T.Y., Zhang, J., Zhan, K.Y., Zhang, Z.L., He, J. Y., 2018. Competitive adsorption and diffusion of CH<sub>4</sub>/CO<sub>2</sub> binary mixture within shale organic nanochannels. *J. Nat. Gas Sci. Eng.* 53, 329–336.
- Liu, J., Xie, L.Z., Elsworth, D., Gan, Q., 2019. CO<sub>2</sub>/CH<sub>4</sub> competitive adsorption in shale: implications for enhancement in gas production and reduction in carbon emissions. *Environ. Sci. Technol.* 53, 9328–9336.
- Merkel, A., Gensterblum, Y., Krooss, B.M., Amann, A., 2015. Competitive sorption of CH<sub>4</sub>, CO<sub>2</sub> and H<sub>2</sub>O on natural coals of different rank. *Int. J. Coal Geol.* 150–151, 181–192.
- Mofarahi, M., Bakhtyari, A., 2015. Experimental investigation and thermodynamic modeling of CH<sub>4</sub>/N<sub>2</sub> adsorption on zeolite 13X. *J. Chem. Eng. Data* 60 (3), 683–696.
- Myers, A.L., 2004. Characterization of nanopores by standard enthalpy and entropy of adsorption of probe molecules. *Colloid. Surface. A* 241, 9–14.
- Nie, B.S., He, X.Q., Wang, E.Y., 2000. Surface free energy of coal and its calculation. *J. Taiyuan Univ. Technol.* 31 (4), 346–348.
- Ning, P., Li, F.R., Yi, H.H., Tang, X.L., Peng, J.H., Li, Y.D., He, D., Deng, H., 2012. Adsorption equilibrium of methane and carbon

- dioxide on microwave-activated carbon. *Sep. Purif. Technol.* 98, 321–326.
- Pei, P., Ling, K., He, J., Liu, Z.Z., 2015. Shale gas reservoir treatment by a CO<sub>2</sub>-based technology. *J. Nat. Gas Sci. Eng.* 26, 1595–1606.
- Qin, C., Jiang, Y.D., Zhou, J.P., Zuo, S.Y., Chen, S.W., Liu, Z.J., Yin, H., Li, Y., 2021a. Influence of supercritical CO<sub>2</sub> exposure on water wettability of shale: Implications for CO<sub>2</sub> sequestration and shale gas recovery. *Energy*. <https://doi.org/10.1016/j.energy.2021.122551>.
- Qin, C., Jiang, Y.D., Zuo, S.Y., Chen, S.W., Xiao, S.Y., Liu, Z.J., 2021b. Investigation of adsorption kinetics of CH<sub>4</sub> and CO<sub>2</sub> on Yanchang shale exposure to supercritical CO<sub>2</sub>. *Energy* 236, 121410.
- Ridha, F.N., Webley, P.A., 2010. Entropic effects and isosteric heats of nitrogen and carbon dioxide adsorption on chabazite zeolites. *Micropor. Mesopor. Mat.* 132, 22–30.
- Sircar, S., 1991. Isosteric heats of multicomponent gas adsorption on heterogeneous adsorbents. *Langmuir* 7, 3065–3069.
- Sircar, S., 1992. Estimation of isosteric heats of adsorption of single gas and multicomponent gas mixtures. *Ind. Eng. Chem. Res.* 31, 1813–1819.
- Song, X., Wang, L.A., Ma, X., Zeng, Y.M., 2017. Adsorption equilibrium and thermodynamics of CO<sub>2</sub> and CH<sub>4</sub> on carbon molecular sieves. *Appl. Surf. Sci.* 396, 870–878.
- Song, Z.P., Zhang, B., Kang, T.H., 2018. Molecular simulation of CO<sub>2</sub>/CH<sub>4</sub> competitive adsorption in kaolinite based on adsorption potential theory. *Bull. Mineral., Petrol. Geochem.* 37 (4), 724–730.
- Tang, X., Ripepi, N., Luxbacher, K., Pitcher, E., 2017. Adsorption models for methane in shale: review, comparison, and application. *Energy Fuel* 31 (10), 10787–10801.
- Tang, X., Wang, Z.F., Ripepi, N., Kang, B., Yue, G.W., 2015. Adsorption affinity of different types of coal: mean isosteric heat of adsorption. *Energy Fuel* 29, 3609–3615.
- Van, Ness H.C., 1969. Adsorption of gases on solids. Review of role of thermodynamics. *Ind. Eng. Chem. Fundamen.* 8 (3), 464–473.
- Wang, Q., Huang, L., 2019. Molecular insight into competitive adsorption of methane and carbon dioxide in montmorillonite: effect of clay structure and water content. *Fuel* 239, 32–43.
- Wang, T.Y., Tian, S.C., Li, G.S., Sheng, M., Ren, W.X., Liu, Q.L., Zhang, S.K., 2018. Molecular simulation of CO<sub>2</sub>/CH<sub>4</sub> competitive adsorption on shale kerogen for CO<sub>2</sub> sequestration and enhanced gas recovery. *J. Phys. Chem. C* 122, 17009–17018.
- Wang, Q.Q., Zhang, D.F., Wang, H.H., Jiang, W.P., Wu, X.P., Yang, J., Huo, P.L., 2015. Influence of CO<sub>2</sub> exposure on high-pressure methane and CO<sub>2</sub> adsorption on various rank coals: implications for CO<sub>2</sub> sequestration in coal seams. *Energy Fuel* 29, 3785–3795.
- Xiong, J., Liu, X.J., Liang, L.X., Zeng, Q., 2017. Adsorption behavior of methane on kaolinite. *Ind. Eng. Chem. Res.* 56 (21), 6229–6238.
- Xue, P., Gao, D.C., Sun, J.B., Zhang, L.X., Qi, P.W., Shi, P., 2018. Adsorption thermodynamic property of Yangchang formation shale in Ordos basin. *Coal Geol. Exploration* 46 (4), 22–27.
- Zhang, B., Kang, J.T., Kang, T.H., 2018. Effect of water on methane adsorption on the kaolinite (001) surface based on molecular simulations. *Appl. Surf. Sci.* 439, 792–800.
- Zhao, P., Xie, L.Z., He, B., Liu, J., 2020. Strategy optimization on industrial CO<sub>2</sub> sequestration in the depleted Wufeng-Longmaxi formation shale in the Northeastern Sichuan basin, SW China: from the perspective of environment and energy. *ACS Sustain. Chem. Eng.* 8 (30), 11435–11445.
- Zhou, L., Feng, Q.Y., Qin, Y., 2011. Thermodynamic analysis of competitive adsorption of CO<sub>2</sub> and CH<sub>4</sub> on coal matrix. *J. China Coal Soc.* 36 (8), 1307–1311.
- Zhou, W.N., Wang, H.B., Yang, Y.Y., Liu, X.L., 2019. Adsorption mechanism of CO<sub>2</sub>/CH<sub>4</sub> in kaolinite clay: insight from molecular simulation. *Energy Fuel* 33, 6542–6551.
- Zhou, X., Yi, H.H., Tang, X.L., Deng, H., Liu, H.Y., 2012. Thermodynamics for the adsorption of SO<sub>2</sub>, NO and CO<sub>2</sub> from flue gas on activated carbon fiber. *Chem. Eng. J.* 200–202, 399–404.